



Publication Year	2005
Acceptance in OA @INAF	2023-02-21T14:18:28Z
Title	LFI Main Beams at 70 GHz
Authors	SANDRI, MAURA; VILLA, Fabrizio
Handle	http://hdl.handle.net/20.500.12386/33689
Number	PL-LFI-PST-TN-062



TITLE: LFI Main Beams at 70 GHz


DOC. TYPE: TECHNICAL NOTE

PROJECT REF.: PL-LFI-PST-TN-062

PAGE: I of V, 14

ISSUE/REV.: 1.0

DATE: February 2005

Prepared by	M. SANDRI F. VILLA LFI Project System Team	Date: February 22 th , 2005 <i>Maura Sandri</i> Signature:  _____
Agreed by	C. BUTLER LFI Program Manager	Date: February 22 th , 2005 <i>R.C. Butler</i> Signature: _____
Approved by	N. MANDOLESI LFI Principal Investigator	Date: February 22 th , 2005 <i>N. Mandolesi</i> Signature: _____



DISTRIBUTION LIST

Recipient	Company / Institute	E-mail address	Sent
M.BERSANELLI	Univ. Di Milano – Milano	bersanelli@uni.mi.astro.it	
C.BURIGANA	IASF/CNR – Sezione di Bologna	burigana@bo.iasf.cnr.it	
R.C.BUTLER	IASF/CNR – Sezione di Bologna	butler@bo.iasf.cnr.it	
N.MANDOLESI	IASF/CNR – Sezione di Bologna	mandolesi@bo.iasf.cnr.it	
A.MENNELLA	IASF/CNR – Sezione di Milano	daniele@mi.iasf.cnr.it	
M.SANDRI	IASF/CNR – Sezione di Bologna	sandri@bo.iasf.cnr.it	
J.TAUBER	ESA / ESTEC – Noordwijk	jtauber@rssd.esa.int	
F.VILLA	IASF/CNR – Sezione di Bologna	villa@bo.iasf.cnr.it	
F.PASIAN	OAT – Trieste	pasian@ts.astro.it	
LFISPCC		lfispcc@bo.iasf.cnr.it	



CHANGE RECORD

Issue	Date	Sheet	Description of Change	Release
1.0	22/02/05	All	First issue of the document	==



USEFUL ACRONYMS

Acronym	Description
GO	Geometrical Optics
GTD	Geometrical Theory of Diffraction
PO	Physical Optics
PTD	Physical Theory of Diffraction
RDP	Reference Detector Plane
LOS	Line Of Sight
ET	Edge Taper
XPD	X- Polar Discrimination
FWHM	Full Width Half Maximum
HW	Half Width



TABLE OF CONTENTS

1	INTRODUCTION	1
2	THE OPTICS	1
3	MAIN BEAMS.....	2
3.1	MAIN BEAM #18.....	3
3.1.1	X-polarized.....	3
3.1.2	Y-polarized.....	3
3.2	MAIN BEAM #19.....	4
3.2.1	X-polarized.....	4
3.2.2	Y-polarized.....	4
3.3	MAIN BEAM #20.....	5
3.3.1	X-polarized.....	5
3.3.2	Y-polarized.....	5
3.4	MAIN BEAM #21.....	6
3.4.1	X-polarized.....	6
3.4.2	Y-polarized.....	6
3.5	MAIN BEAM #22.....	7
3.5.1	X-polarized.....	7
3.5.2	Y-polarized.....	7
3.6	MAIN BEAM #23.....	8
3.6.1	X-polarized.....	8
3.6.2	Y-polarized.....	8
4	CONCLUSIONS	9
5	REFERENCES	10
6	APPENDIX.....	10
6.1	DIRECTIVITY, XPD, AND DEPOLARIZATION PARAMETER	10
6.2	ANGULAR RESOLUTION OF THE EQUIVALENT SYMMETRIC BEAM.....	11
6.3	MAIN BEAM PARAMETERS DERIVED FROM ELLIPTICAL GAUSSIAN FIT.....	11



1 INTRODUCTION

This note is to present the results of main beam optical simulations carried out for the LFI dual profiled corrugated feed horns at 70 GHz. Both polarizations have been considered for each feed. The simulations have been carried out in the transmitting mode using GRASP8 software package [1]. PO/PTD has been used on both reflectors.

2 THE OPTICS

The location and orientation of the three LFI feed horns at 70 GHz are reported in Tab. 1, in the Reference Detector Plane Coordinate System [2]. The UV– location of the power peak of the corresponding main beams on the sky are listed in Tab. 2, together with the orientation (with respect to the telescope line of sight) of the coordinate systems in which the main beams have been computed [3].

The feed models used in the simulations are Y– axis polarized dual profiled feed horns specified by tabulated pattern values provided by INAF – Osservatorio Astrofisico di Arcetri. The feed horn directivities are about 20 dBi and the ET values are 17 dB at 22°. The X– axis polarized models have been obtained rotating each feed horn around its axis of 90 degrees.

Tab. 1 70 GHz LFI feed horn locations in the Focal Plane Unit (in the Reference Detector Plane coordinate system).

FH #	Location ($X_{RDP}, Y_{RDP}, Z_{RDP}$) [mm,mm,mm]			Orientation ($\theta_{RDP}, \varphi_{RDP}, \psi_{RDP}$) [deg,deg,deg]		
	18	-76.38	-69.37	14.54	11.93	46.04
19	-92.41	-43.29	18.66	11.63	28.71	19.84
20	-101.86	-17.69	20.86	11.38	11.22	21.29
21	-101.86	17.69	20.86	11.38	-11.22	-21.29
22	-92.41	43.29	18.66	11.63	-28.71	-19.84
23	-76.38	69.37	14.54	11.93	-46.04	-18.26

Tab. 2 Main beams locations on the sky ($u = \sin\theta \cdot \cos\varphi$, $v = \sin\theta \cdot \sin\varphi$) and polarization angle, ψ .

MB #	Location		Orientation ($\theta_{LOS}, \varphi_{LOS}, \psi_{LOS}$) [deg,deg,deg]		
	U	V			
18	-0.03835	-0.04287	3.2975	-131.8147	22.3
19	-0.04837	-0.02697	3.1747	-150.8570	22.4
20	-0.05409	-0.01106	3.1649	-168.4438	22.4
21	-0.05409	0.01106	3.1649	168.4438	-22.4
22	-0.04837	0.02697	3.1747	150.8570	-22.4
23	-0.03835	0.04287	3.2975	131.8147	-22.3



3 MAIN BEAMS

Each main beam has been computed in the co- and x- polar basis according to the Ludwig's third definition [4], in spherical grids with 301×301 points ($-0.015 \leq U, V \leq 0.015$). The contour plots are shown in Fig. 1 – Fig. 12. The contour lines plotted are the levels at $-3, -6, -10, -20, -30, -40, -50, -60$, and -70 dB from the corresponding power peak. The colour scale goes from -90 to 0 dB.

The simulations have been carried out in the transmitting mode using GRASP8. PO/PTD has been used on both reflectors. Correct values for $po1$ and $po2$ used in the primary and secondary reflectors have been determined using an automatic optimization procedure expressly written for PLANCK LFI¹ and they are reported in .

Tab. 3 Po points used in the simulations (ptd points used are always equal to $po2$).

Beam	Pol	Sub Reflector		Main Reflector	
		$po1$	$po2$	$po1$	$po2$
18 – 23	X	320	640	320	1280
18 – 23	Y	320	640	320	1280
19 – 22	X	320	640	320	1280
19 – 22	Y	320	640	320	1280
20 – 21	X	320	640	320	1280
20 – 21	Y	320	640	320	1280

¹ The procedure iteratively changes the GRASP8 input file doubling the po value (first of all $po1$ and then $po2$ on the sub reflector, then $po1$ and $po2$ on the main reflector) and computes the main beam. This doubling of po points is continued until the main reflector field is converged, i.e. until the point-to-point comparison between the field computed at the N iteration (normalised to the maximum value found in the main beam grid) differs at the most of $E^{C/20}$ from which obtained at the $(N-1)$ iteration, where C is the convergency level that defines the required accuracy of the calculations. In this condition the field obtained using the $po1$ and $po2$ values is the same (within the convergency level) of that obtained doubling the po values. The convergency level assumed in the PLANCK optical simulations is a factor E^{-4} in the normalised power amplitude of the field. This means that the field error due to convergence is at least 80 dB below the maximum value of the field on any of the field points, and it corresponds to ± 1 dB at -60 dB level that is less than the accuracy required in the main beam measurements.



3.1 Main Beam #18

3.1.1 X- polarized

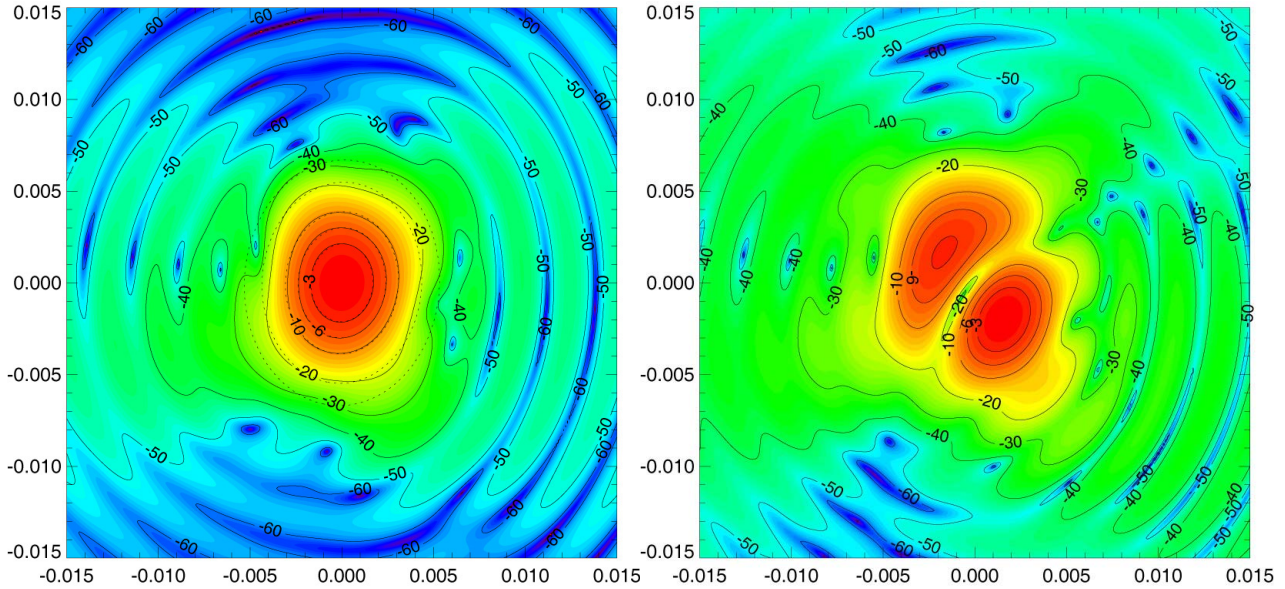


Fig. 1 UV- plot of the co- and x- polar components of LFI18 at 70 GHz, X- axis polarized.

3.1.2 Y- polarized

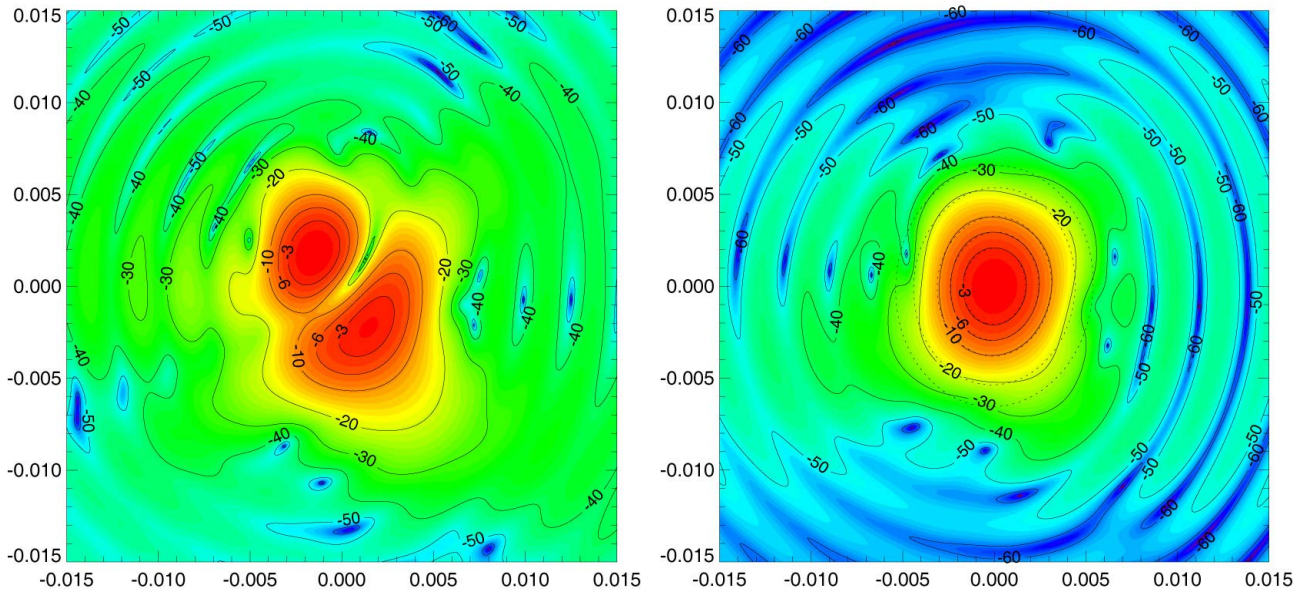


Fig. 2 UV- plot of the x- and co- polar components of LFI18 at 70 GHz, Y- axis polarized.



3.2 Main Beam #19

3.2.1 X- polarized

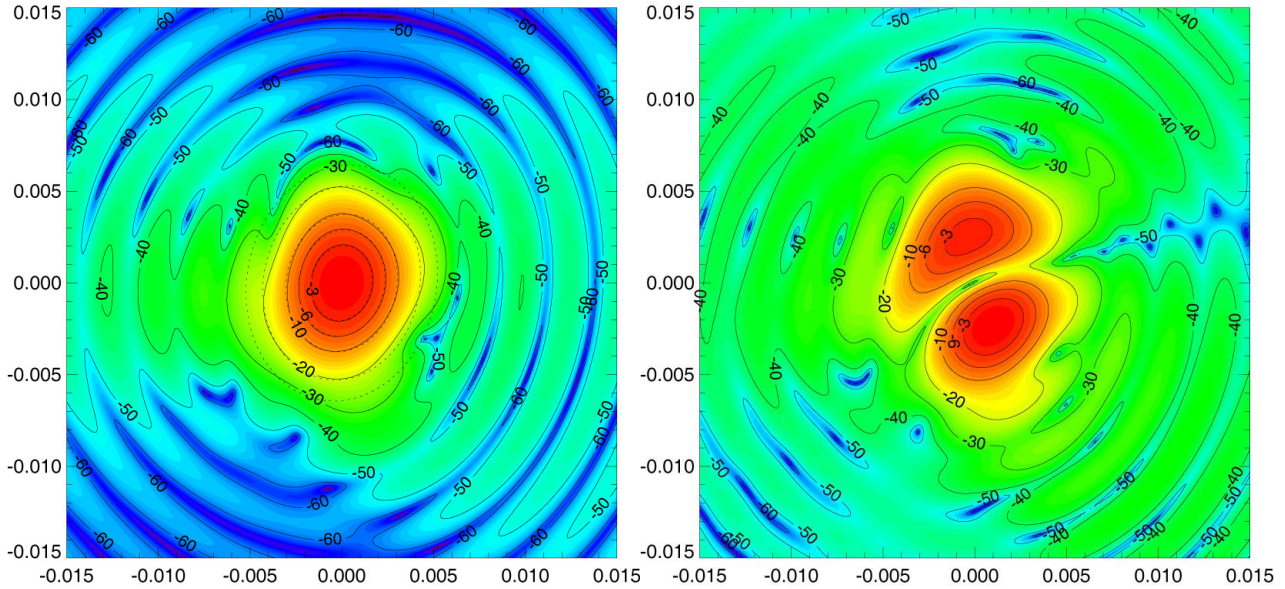


Fig. 3 UV- plot of the co- and x- polar components of LFI19 at 70 GHz, X- axis polarized.

3.2.2 Y- polarized

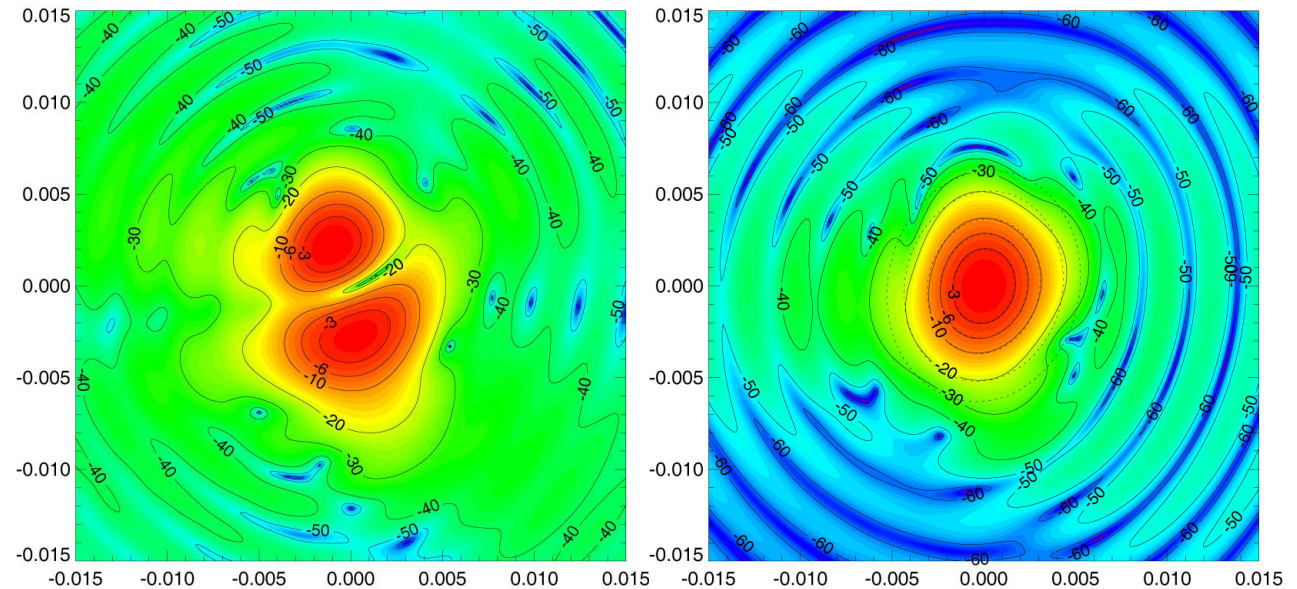


Fig. 4 UV- plot of the x- and co- polar components of LFI19 at 70 GHz, Y- axis polarized.



3.3 Main Beam #20

3.3.1 X- polarized

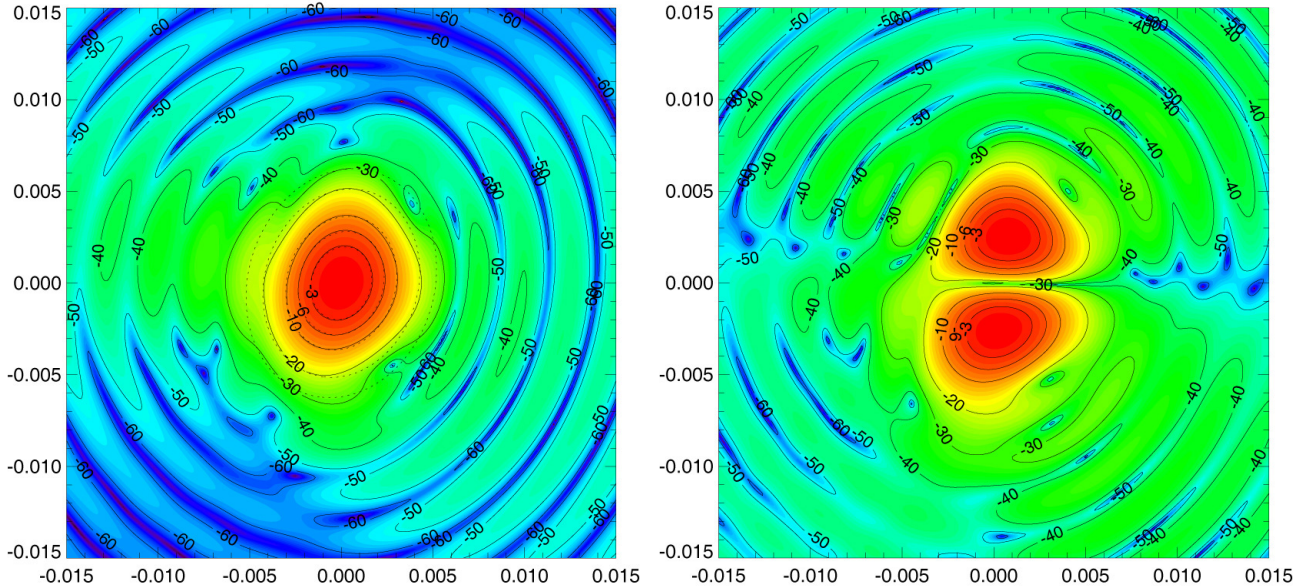


Fig. 5 UV- plot of the co- and x- polar components of LFI20 at 70 GHz, X- axis polarized.

3.3.2 Y- polarized

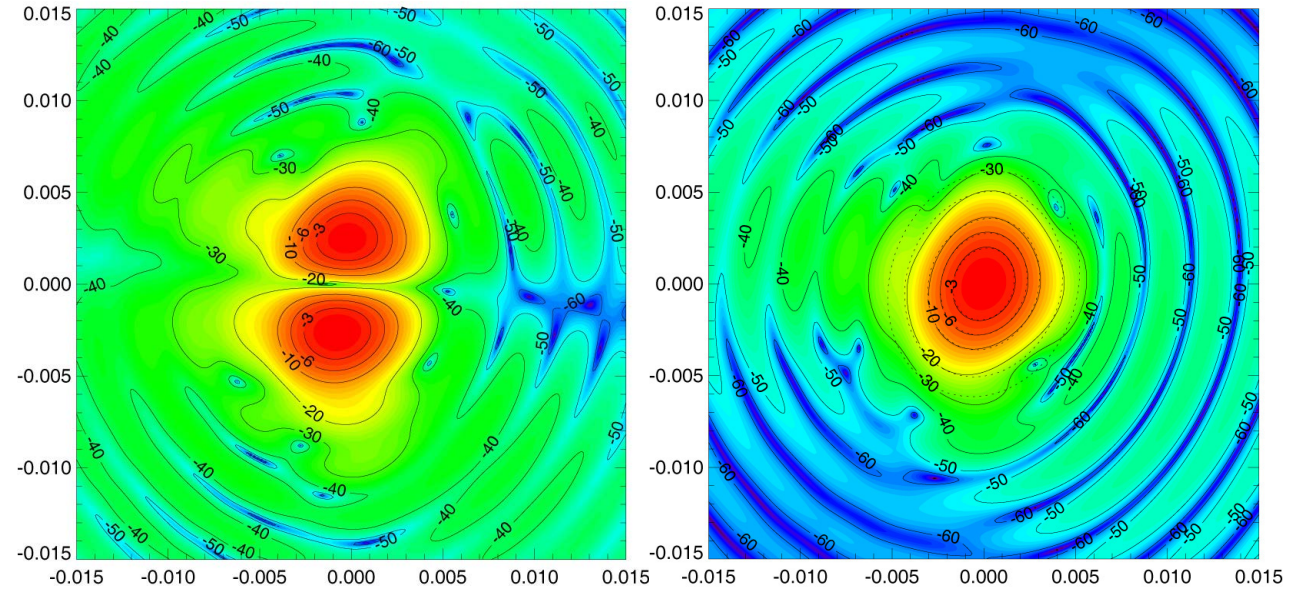


Fig. 6 UV- plot of the x- and co- polar components of LFI20 at 70 GHz, Y- axis polarized.



3.4 Main Beam #21

3.4.1 X- polarized

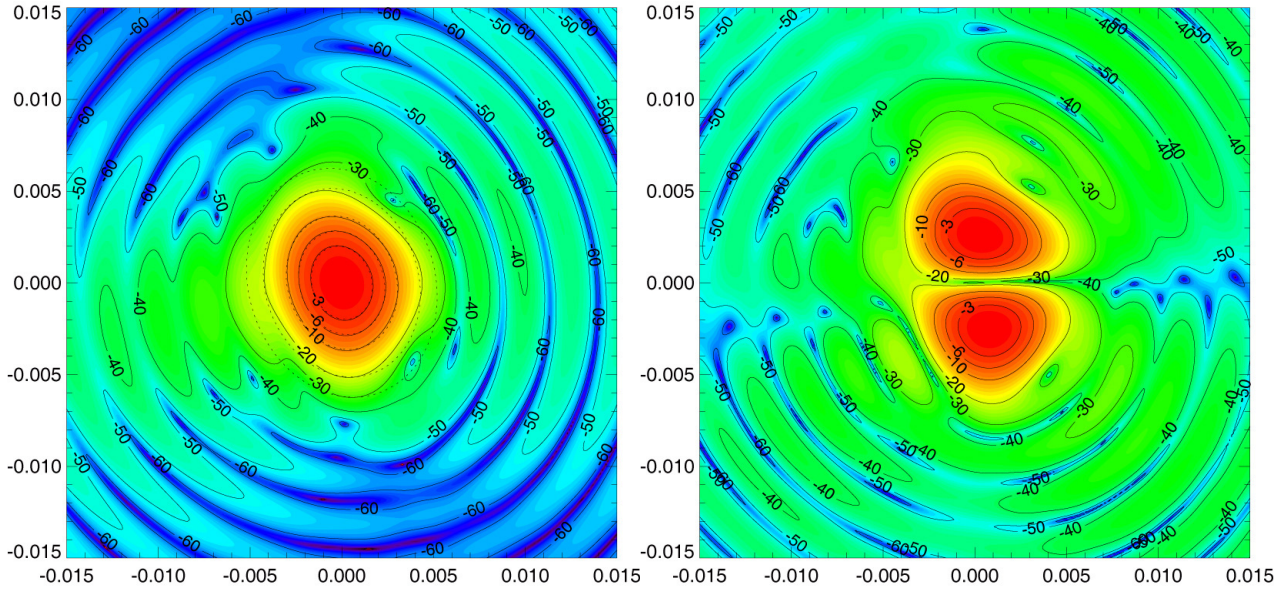


Fig. 7 UV- plot of the co- and x- polar components of LFI21 at 70 GHz, X- axis polarized.

3.4.2 Y- polarized

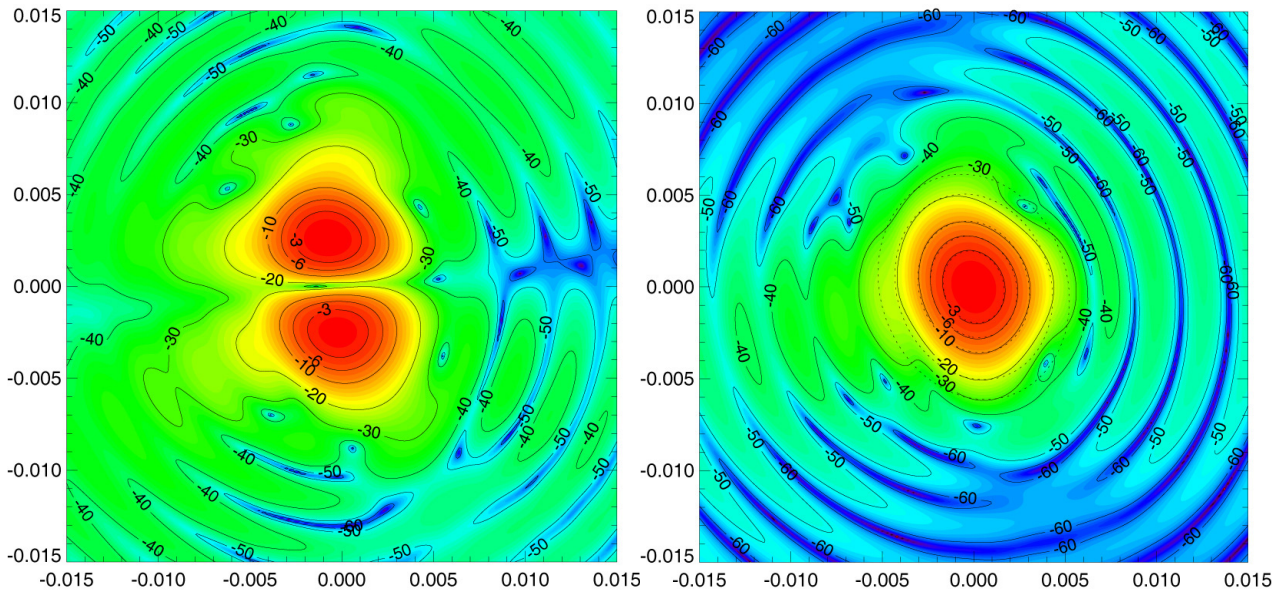


Fig. 8 UV- plot of the x- and co- polar components of LFI21 at 70 GHz, Y- axis polarized.



3.5 Main Beam #22

3.5.1 X- polarized

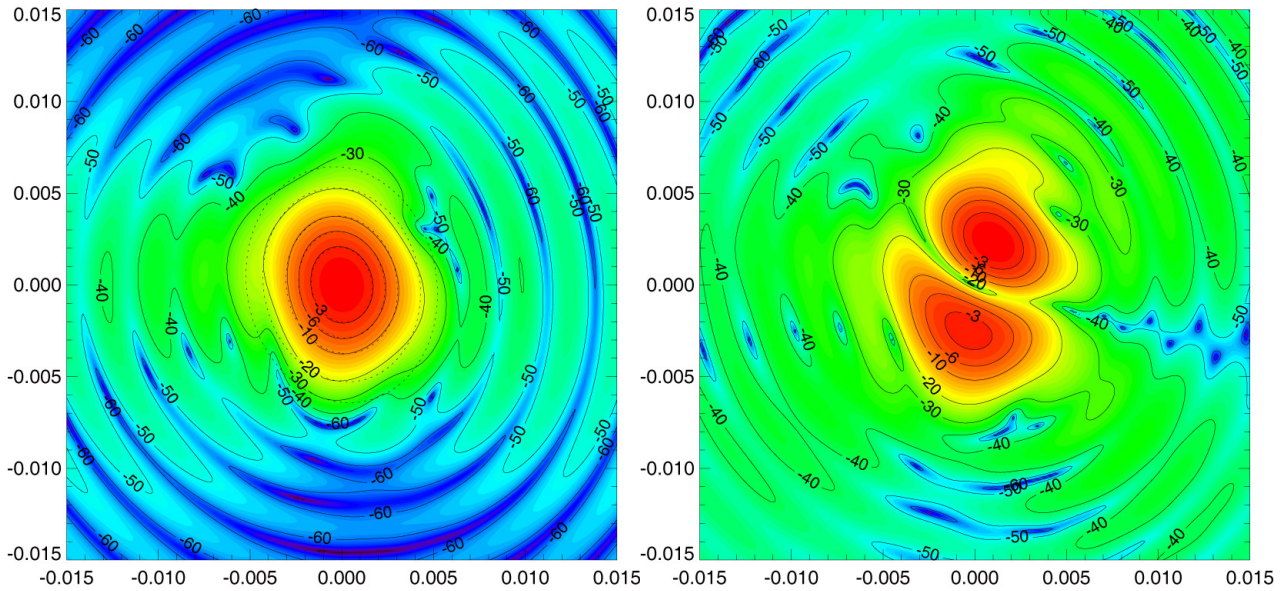


Fig. 9 UV- plot of the co- and x- polar components of LFI22 at 70 GHz, X- axis polarized.

3.5.2 Y- polarized

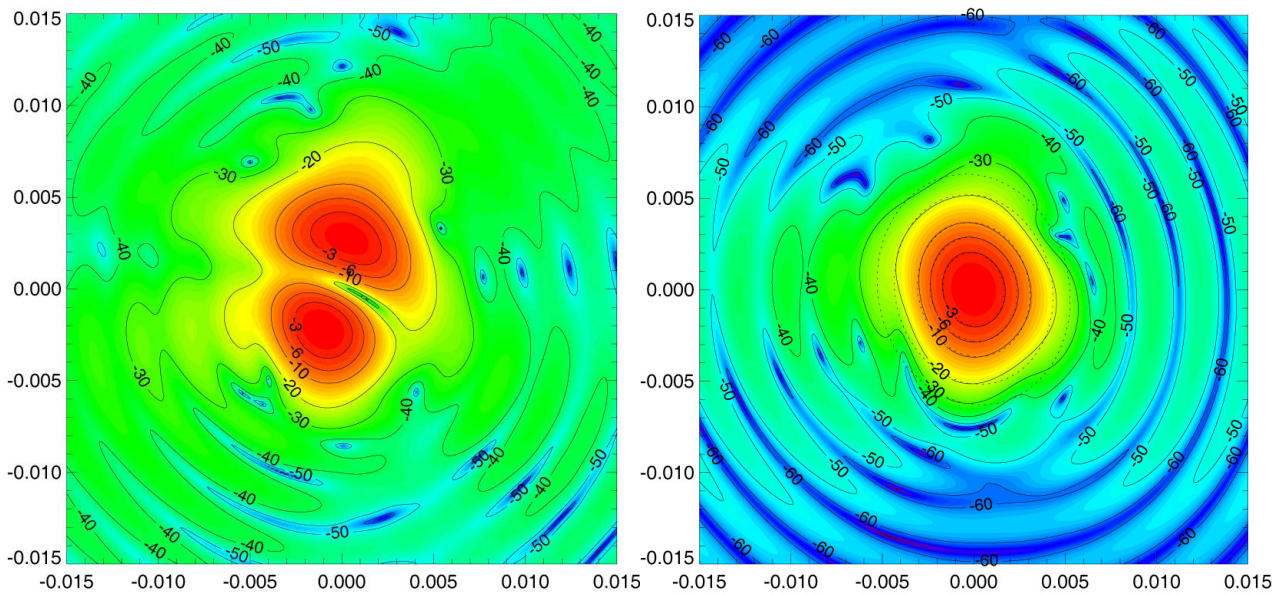


Fig. 10 UV- plot of the x- and co- polar components of LFI22 at 70 GHz, Y- axis polarized.



3.6 Main Beam #23

3.6.1 X- polarized

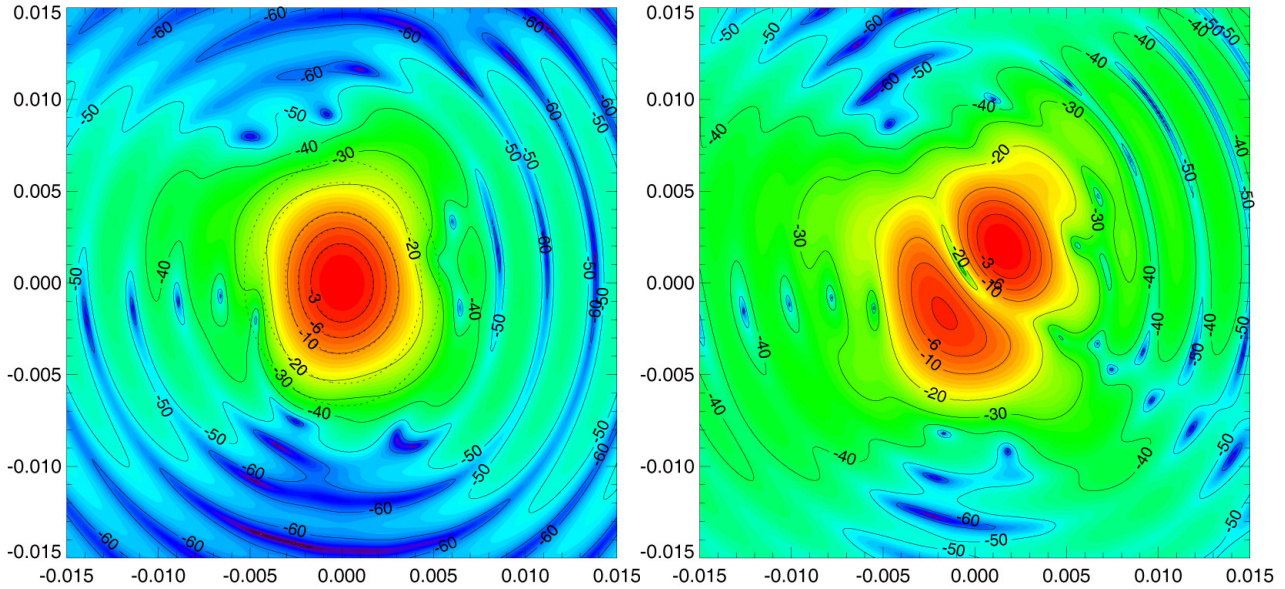


Fig. 11 UV- plot of the co- and x- polar components of LFI23 at 70 GHz, X- axis polarized.

3.6.2 Y- polarized

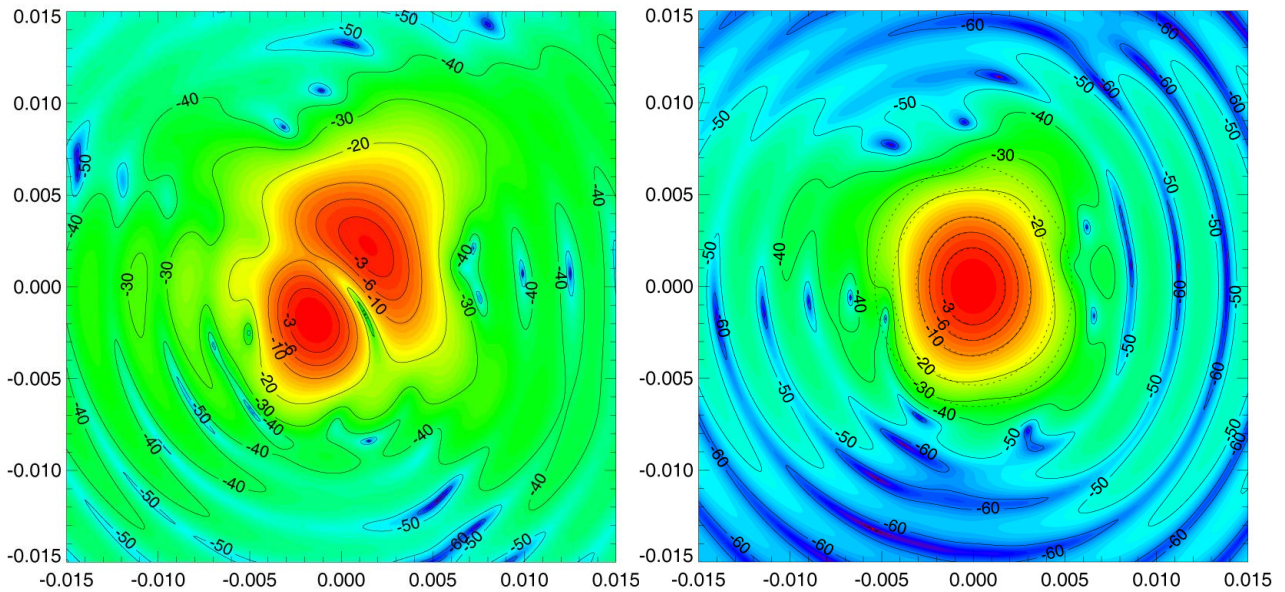


Fig. 12 UV- plot of the x- and co- polar components of LFI23 at 70 GHz, Y- axis polarized.



4 CONCLUSIONS

The 70 GHz LFI main beams have been computed for dual profiled corrugated feed horns (#18, #19, #20, #21, #22, and #23) coupled with the PLANCK telescope. The results are reported in Tab. 4, for both polarizations.

Tab. 4 Main beam characteristics. The HW (minimum and maximum, columns 6 ÷ 11) and the beam solid angle (columns 14 ÷ 16) at -3, -10, -20 dB are also reported. FWHM (column 12) is the average value between the minimum and maximum of the beam width at -3 dB. The cross polar discrimination factor (XPD, column 5), the main beam depolarisation (d , column 13), and the angular resolution of the symmetric beam with the same beam area at a level of -3 dB (column 17) are reported, as computed in 6.1 and 6.2.

MB #	Pol	Co-polar max (dBi)	X-polar max (dBi)	XPD	HW @ -3 dB (deg)	HW @ -10 dB (deg)	HW @ -20 dB (deg)	FWHM (arcmin)	d (%)	Ω_{-3dB} (sr)	Ω_{-10dB} (sr)	Ω_{-20dB} (sr)	θ_{-3dB} (arcmin)
18	X	58.80	30.79	28.01	0.0969	0.1235	0.1702	0.2212	0.3147	0.116E-04	0.373E-04	0.743E-04	13.21
18	Y	58.83	30.29	28.54	0.0989	0.1219	0.1725	0.2176	0.3096	0.115E-04	0.370E-04	0.737E-04	13.15
19	X	59.02	29.29	29.73	0.0969	0.1219	0.1667	0.2167	0.3013	0.111E-04	0.353E-04	0.679E-04	12.92
19	Y	59.06	28.86	30.21	0.0969	0.1187	0.1690	0.2131	0.2967	0.111E-04	0.350E-04	0.672E-04	12.92
20	X	59.17	27.97	31.20	0.0949	0.1203	0.1643	0.2140	0.2981	0.108E-04	0.340E-04	0.644E-04	12.75
20	Y	59.22	28.23	30.99	0.0949	0.1187	0.1655	0.2112	0.2941	0.107E-04	0.337E-04	0.635E-04	12.69
21	X	59.17	27.97	31.20	0.0949	0.1203	0.1643	0.2140	0.2981	0.108E-04	0.340E-04	0.644E-04	12.75
21	Y	59.22	28.23	30.99	0.0949	0.1187	0.1655	0.2112	0.2941	0.107E-04	0.337E-04	0.635E-04	12.69
22	X	59.02	29.29	29.73	0.0969	0.1219	0.1667	0.2167	0.3013	0.111E-04	0.353E-04	0.679E-04	12.92
22	Y	59.06	28.86	30.21	0.0969	0.1187	0.1690	0.2131	0.2967	0.111E-04	0.350E-04	0.672E-04	12.92
23	X	58.80	30.79	28.01	0.0969	0.1235	0.1702	0.2212	0.3147	0.116E-04	0.373E-04	0.743E-04	13.21
23	Y	58.83	30.29	28.54	0.0989	0.1219	0.1725	0.2176	0.3096	0.115E-04	0.370E-04	0.737E-04	13.15



5 REFERENCES

- [1] K. Pontoppidan, *Technical Description of GRASP8*, TICRA, Doc.No.S-894-02, 1999.
[2] FIRST/PLANCK Project, *PLANCK Telescope Design Specification*, SCI-PT-RS-07024.
[3] M. Sandri and F. Villa, *PLANCK/LFI: Main Beam Locations and Polarization Alignment for the LFI baseline FPU*, PL-LFI-ST-TN-027, 2001.
[4] A. C. Ludwig, *The Definition of Cross Polarization*, IEEE Transactions on Antennas and Propagation, pp.116-119, Jan 1973.

6 APPENDIX

6.1 Directivity, XPD, and Depolarization Parameter

The directivity of the copolar (D_{cp}) and cross-polar (D_{xp}) components have been computed. Then the cross polar discrimination factor (XPD)² has been obtained:

$$XPD = \frac{D_{xp}}{D_{cp}}$$

The depolarization parameter has been obtained in the following way. The Stokes parameters have been computed for each beam, in each point of the regular (u, v) grid.

$$\begin{aligned} S_I(u, v) &= E_{cp}(u, v)^2 + E_{xp}(u, v)^2 \\ S_Q(u, v) &= E_{cp}(u, v)^2 - E_{xp}(u, v)^2 \\ S_U(u, v) &= 2 \cdot E_{cp}(u, v) \cdot E_{xp}(u, v) \cdot \cos[\delta\varphi(u, v)] \\ S_V(u, v) &= 2 \cdot E_{cp}(u, v) \cdot E_{xp}(u, v) \cdot \sin[\delta\varphi(u, v)] \end{aligned}$$

in which $E_{cp}(u, v)$ and $E_{xp}(u, v)$ are the amplitude field of the co- polar and x- polar components respectively, $\delta\varphi$ is the phase difference between the co- polar and x- polar fields. Then, over the whole (u, v) plane calculated each parameter has been summed.

$$S_N = \sum_{(u,v)} S_N(u, v) \cdot \Delta u \Delta v, N = I, Q, U, V$$

and finally

$$Dep\% = \left(1 - \frac{\sqrt{S_Q^2 + S_U^2 + S_V^2}}{S_I} \right) \cdot 100.$$

² This ratio is improperly called XPD. Actually the cross polar discrimination is calculated punctually as the ratio between the x- polar and the co- polar component. Then the XPD is a function of (u, v) coordinates. In this case the XPD is an indication of the maximum x- polar level normalized to the co- polar peak.



6.2 Angular Resolution of the Equivalent Symmetric Beam

The angular resolution as been calculated also from the contour area at -3 dB, $\Omega_{-3\text{dB}}$ reported in Tab. 4, the latter obtained by the GRASP8 post processor. For a circular beam, the area within the equivalent FWHM (named $\theta_{-3\text{dB}}$ in Tab. 4) can be computed as follows:

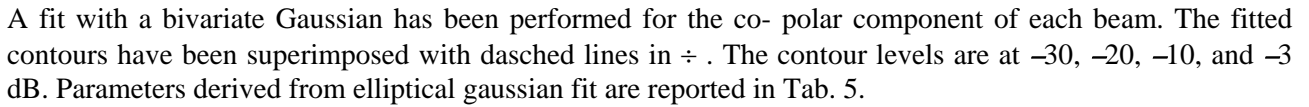
$$\begin{aligned}\Omega_{\text{FWHM}} &= \int_0^{2\pi} \int_0^{\text{FWHM}/2} \sin \theta \cdot d\theta \cdot d\phi = \\ &= 2\pi \cdot \left[1 - \cos \frac{\text{FWHM}}{2} \right]\end{aligned}$$

Then,

$$\text{FWHM} = 2 \cdot \text{acos} \left(1 - \frac{\Omega_{\text{FWHM}}}{2\pi} \right)$$

If $\Omega_{\text{FWHM}} = \Omega_{-3\text{dB}}$ we can easily calculate the angular resolution of the symmetric beam with the same beam area.

6.3 Main beam parameters derived from elliptical gaussian fit

A fit with a bivariate Gaussian has been performed for the co- polar component of each beam. The fitted contours have been superimposed with dashed lines in . The contour levels are at -30 , -20 , -10 , and -3 dB. Parameters derived from elliptical gaussian fit are reported in Tab. 5.

Tab. 5 Parameters derived from elliptical gaussian fit. The tilt angle is defined with respect to the X- axis of the main beam coordinate system (defined in Tab. 2 with respect to the LOS frame), in the clockwise direction.

MB #	Pol	FWHM (arcmin)			tilt (degree)
		min	max	ave	
18	X	11.61	14.63	13.12	3.36
18	Y	11.77	14.34	13.05	3.92
19	X	11.36	14.21	12.79	10.58
19	Y	11.47	13.95	12.71	12.06
20	X	11.18	13.93	12.56	16.95
20	Y	11.24	13.74	12.49	18.72
21	X	11.18	13.93	12.56	-16.95
21	Y	11.24	13.74	12.49	-18.72
22	X	11.36	14.21	12.79	-10.58
22	Y	11.47	13.95	12.71	-12.06
23	X	11.61	14.63	13.12	-3.36
23	Y	11.77	14.34	13.05	-3.92

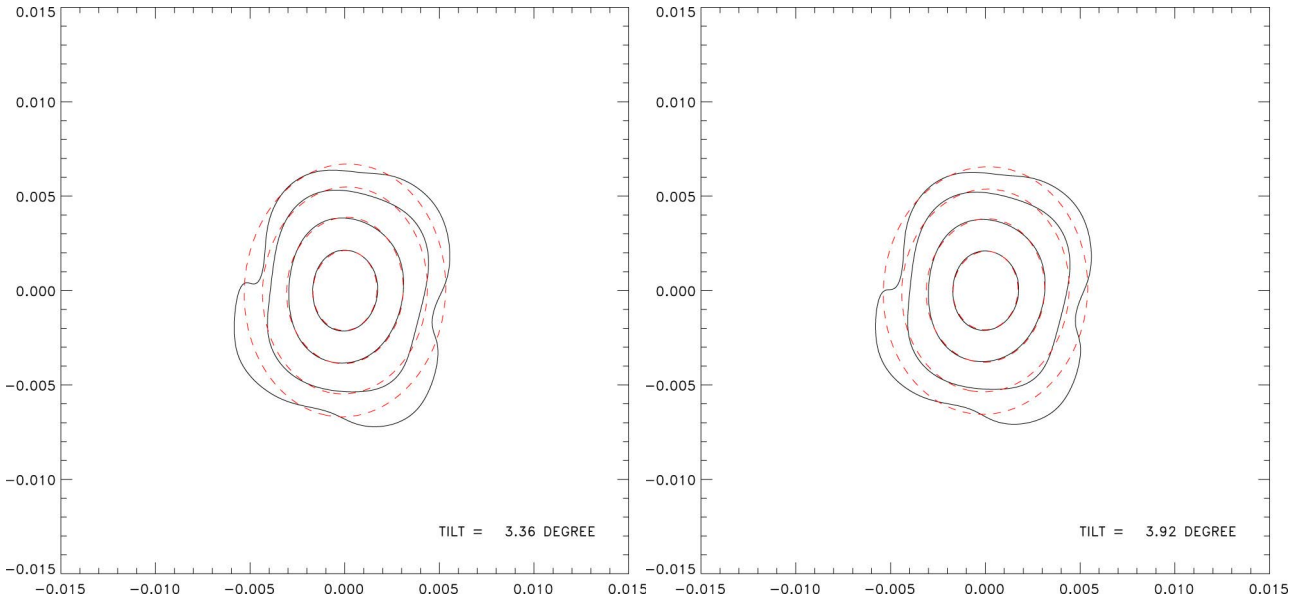


Fig. 13 Main beam #18 X (left side) and Y (right side) polarized

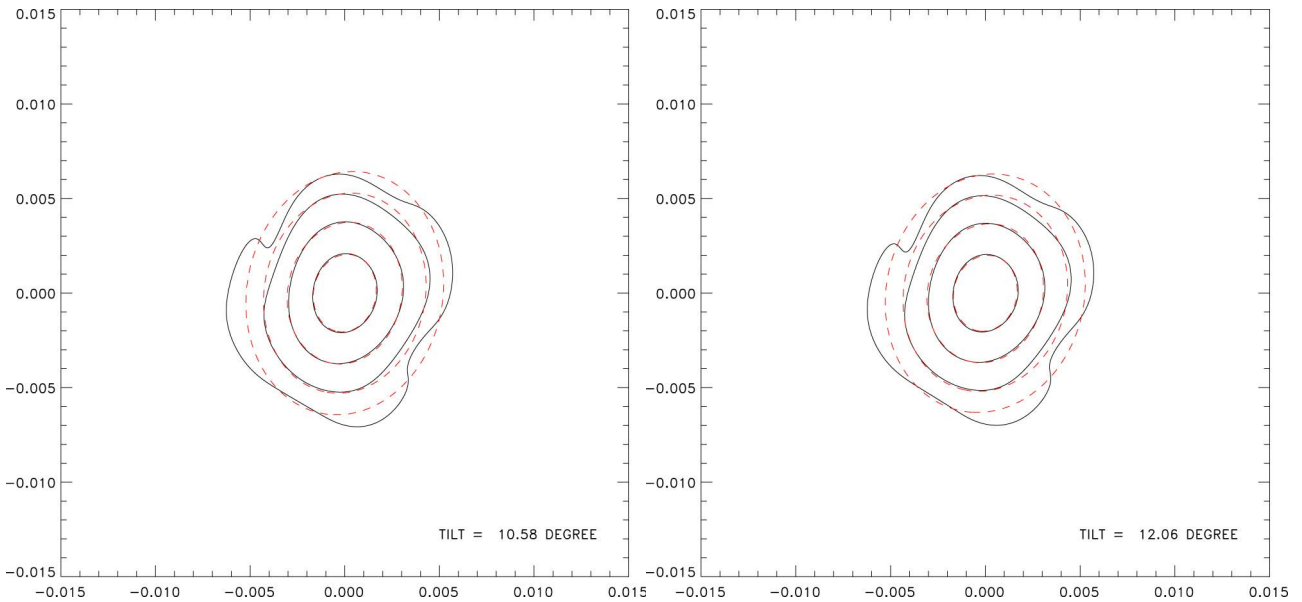


Fig. 14 Main beam #19 X (left side) and Y (right side) polarized

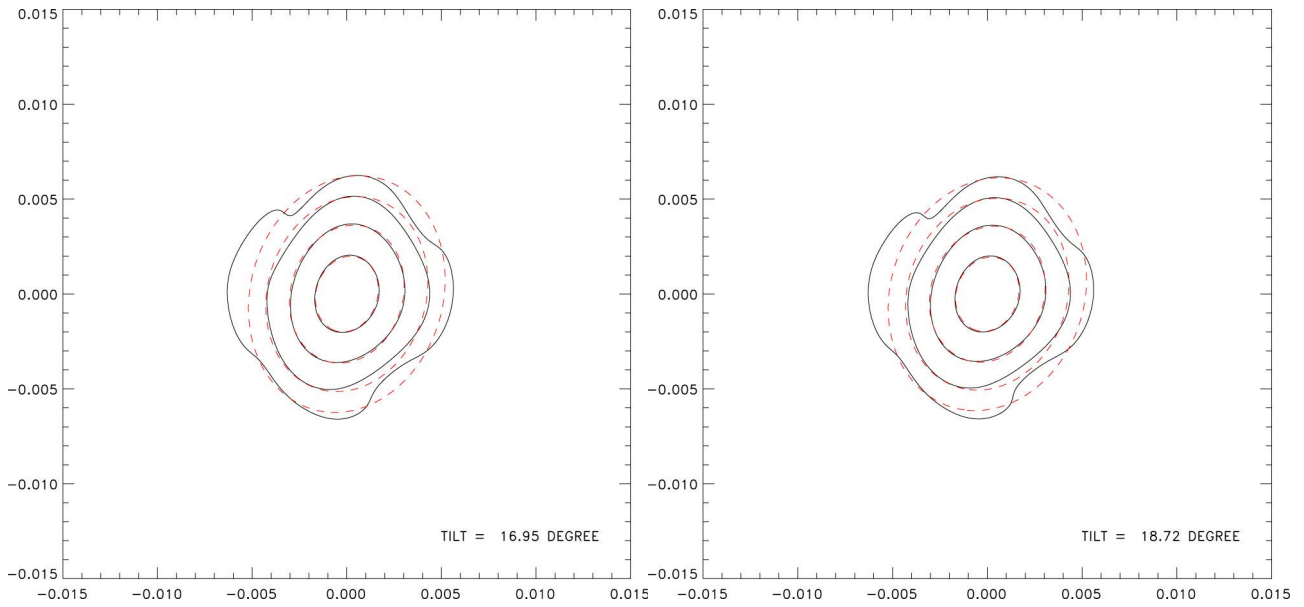


Fig. 15 Main beam #20 X (left side) and Y (right side) polarized

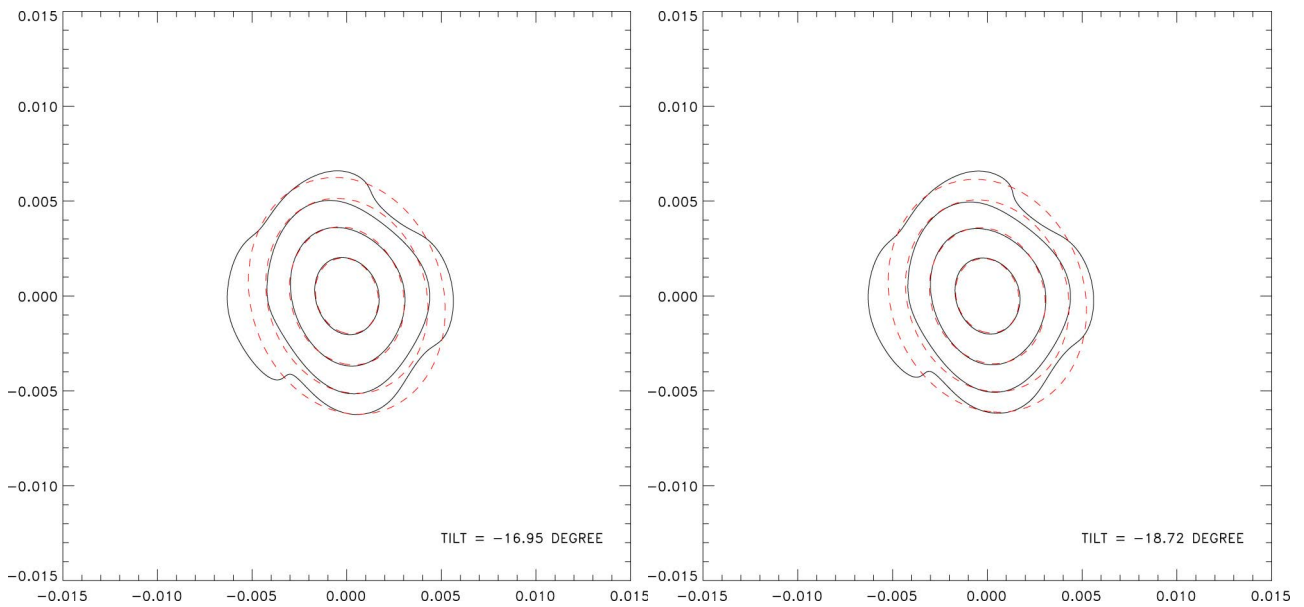


Fig. 16 Main beam #21 X (left side) and Y (right side) polarized

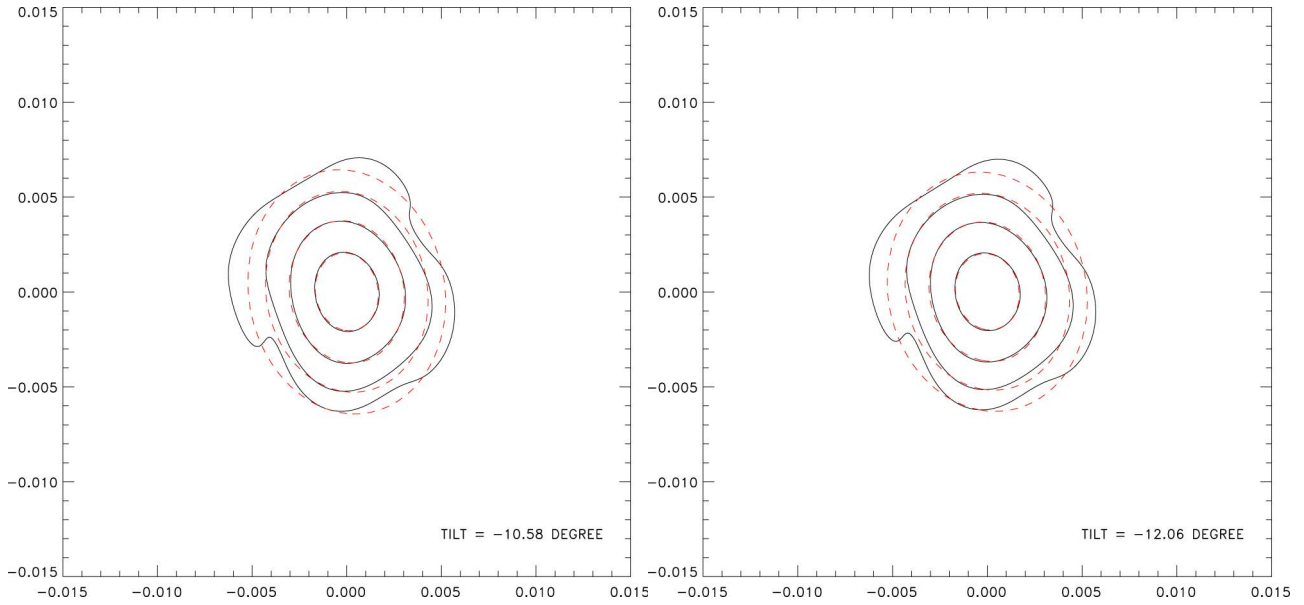


Fig. 17 Main beam #22 X (left side) and Y (right side) polarized

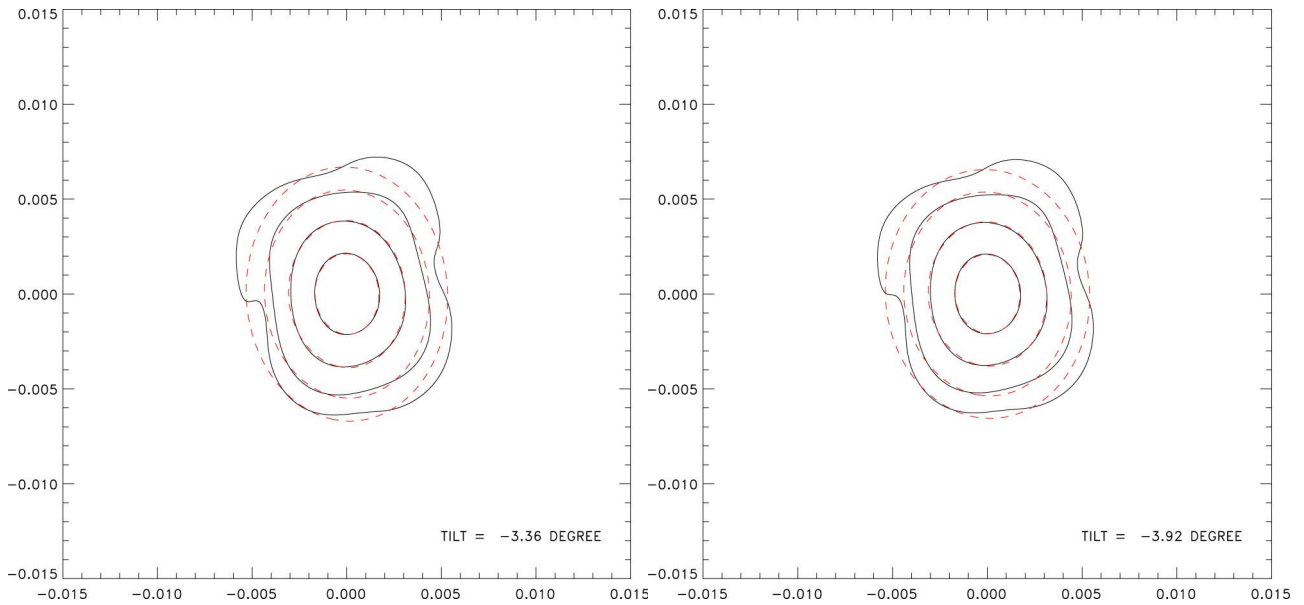


Fig. 18 Main beam #23 X (left side) and Y (right side) polarized